

Flavor Structure of the Nucleon Sea from Lattice QCD

Huey-Wen Lin,^{1,*} Jiunn-Wei Chen,^{2,†} Saul D. Cohen,^{3,1,‡} and Xiangdong Ji^{4,5,§}

¹*Department of Physics, University of Washington, Seattle, WA 98195-1560*

²*Department of Physics, National Center for Theoretical Sciences,
and Leung Center for Cosmology and Particle Astrophysics,
National Taiwan University, Taipei 10617, Taiwan*

³*Institute for Nuclear Theory, University of Washington, Seattle, WA 98195-1560*

⁴*Maryland Center for Fundamental Physics, Department of Physics,
University of Maryland, College Park, Maryland 20742, USA*

⁵*INPAC, Department of Physics and Astronomy,
Shanghai Jiao Tong University, Shanghai, 200240, P. R. China*

(Dated: February 23, 2015)

We present the first direct lattice calculation of the isovector sea-quark distributions in the nucleon within the framework of the large-momentum effective field theory proposed recently. We use $N_f = 2 + 1 + 1$ HISQ lattice gauge ensembles (generated by MILC Collaboration) and clover valence fermions with pion mass 310 MeV. We establish the convergence of the result as the nucleon momentum increases within the uncertainty of the calculation. Although the lattice systematics are not yet fully under control, we obtain some qualitative features of the flavor structure of the nucleon sea: $\bar{d}(x) > \bar{u}(x)$ leading to the violation of the Gottfried sum rule; $\Delta\bar{u}(x) > \Delta\bar{d}(x)$ as indicated by the STAR data at large and small leptonic pseudorapidity.

PACS numbers: 12.38.Gc, 14.20.Dh, 14.65.Bt

The proton has the quantum numbers of two up and one down quarks. The fundamental theory for the proton structure, quantum chromodynamics (QCD), predicts that in addition to these valence quarks, there is also a sea of quark-antiquark pairs. The antiquarks in the proton can be probed in high-energy scattering, particularly through the Drell-Yan process and similar processes such as W production. They can also be extracted through semi-inclusive processes by tagging the fragmentations of the antiquarks. In recent years, much progress has been made in understanding the flavor structure of the nucleon sea (see Ref. [8] for a recent review), for the unpolarized sea in Drell-Yan [2, 21] and for the polarized sea in semi-inclusive deep-inelastic scattering [5, 9]. Theoretical understanding of the nucleon sea has mostly been from nucleon models [10, 20]. Although the models provide a qualitative physical understanding of the sea, they are not expected to make reliable quantitative predictions. The only fundamental approach to nucleon structure so far is lattice QCD. Unfortunately, the traditional lattice-QCD approach does not allow one to compute the sea directly: one can only calculate lower moments of the parton distributions, which involve quark as well as antiquark contributions, making isolation of the antiquarks difficult.

In a recent paper by one of us [13], a new approach to calculating the full x -dependence of parton physics, such as the parton distributions and other parton observables, has been proposed. The method is based on the observation that, while in the rest frame of the nucleon, parton physics corresponds to light-cone correlations, and the same physics can be obtained through time-independent spatial correlations in the infinite-

momentum frame (IMF). For finite but large momenta feasible in lattice simulations, a large-momentum effective field theory (LaMET) can be used to relate Euclidean quasi-distributions to physical ones through a factorization theorem [14].

In this paper, we report the first attempt to make a lattice calculation of polarized and unpolarized quark distributions using the LaMET formalism. To simplify the computation, we consider only the isovector $u - d$ combination so that the disconnected diagrams do not contribute. We first compute the Euclidean lattice quasi distribution $\tilde{q}_{\text{lat}}(x, \Lambda, P_z)$ at increasing nucleon momentum P_z from 0.43 to 1.29 GeV and then extract the physical light-cone distribution $q(x, \mu)$ by taking into account both one-loop logarithmic and power corrections. The leading power correction arises from the nucleon mass effect in the expansion with respect to $(M_N/4P_z)^2$. We observe the convergence of the result at the largest two nucleon momenta, with small residual corrections coming from dynamical higher-twist effects. Although the final result is not yet entirely physical because of the large light-quark masses, coarse lattice spacing, and lack of complete one-loop matching condition, we nonetheless find a qualitative agreement with experimental data on unpolarized and polarized sea. This demonstrates the feasibility of the approach and will motivate lattice-QCD studies with improved systematics in the future.

For the quark distributions, the starting point is the momentum-dependent nonlocal static correlation

$$\tilde{q}(x, \Lambda, P_z) = \int \frac{dz}{4\pi} e^{-izk} \times \left\langle \vec{P} \left| \bar{\psi}(z) \gamma_z e^{ig \int_0^z A_z(z') dz'} \psi(0) \right| \vec{P} \right\rangle, \quad (1)$$

where $x = k/P_z$, Λ is an ultraviolet (UV) cut-off scale such as $1/a$ on a lattice with a as lattice spacing, \vec{P} is the momentum of the nucleon moving in the z -direction. All fields and couplings are bare and depend on Λ . When the nucleon momentum approaches infinity, the quasi-distribution becomes the physical parton distribution when Λ is fixed. At large but finite P_z , one has an effective field theory expansion [22]

$$\tilde{q}(x, \Lambda, P_z) = \int \frac{dy}{|y|} Z \left(\frac{x}{y}, \frac{\mu}{P_z}, \frac{\Lambda}{P_z} \right) q(y, \mu) + \mathcal{O} \left(\frac{\Lambda_{\text{QCD}}^2}{P_z^2}, \frac{M_N^2}{P_z^2} \right) + \dots \quad (2)$$

where μ is the renormalization scale for the physical parton distribution $q(y)$, usually in $\overline{\text{MS}}$ scheme. The Z function is a perturbation series in α_s , depending among others on the UV properties of the quasi-distribution. Z has been calculated to one-loop order in the transverse-momentum cutoff scheme, but is not yet available in a lattice regularization. As observed in Ref. [17], the above relation can be inverted, since it is perturbative.

In this study, we use clover valence fermions on an ensemble of $24^3 \times 64$ gauge configurations with $a \approx 0.12$ fm, box size $L \approx 3$ fm and pion mass $M_\pi \approx 310$ MeV with $N_f = 2+1+1$ flavors of highly improved staggered quarks (HISQ) generated by MILC Collaboration [6] and apply hypercubic (HYP) smearing [12] to the gauge links. HYP smearing has been shown to significantly improve the discretization effects on operators and shift their corresponding renormalizations toward their tree-level values (near unity for quark bilinear operators) [7]. We calculate the quasi-distributions with long straight gauge-link products between the quark and antiquark in the inserted current,

$$\tilde{q}_{\text{lat}}(x, \Lambda, P_z) = \int \frac{dz}{4\pi} e^{-izk} h(z, \Lambda, P_z),$$

$$h(z, \Lambda, P_z) = \left\langle \vec{P} \left| \bar{\psi}(z) \gamma_z \left(\prod_n U_z(n\hat{z}) \right) \psi(0) \right| \vec{P} \right\rangle, \quad (3)$$

where U_μ is a discrete gauge link in the μ direction.

We generate the results using 1383 measurements (among 461 lattice configurations). We extract the matrix elements $h(z, \Lambda, P_z)$ for various z for our lattice setup with P_z (in units of $2\pi/L$) 1, 2, 3. The statistical error becomes noticeably bigger as the nucleon momentum becomes larger, as typically seen in lattice hadron calculations. The correlation vanishes beyond about 1 fm, as is typical in nonperturbative QCD. This is in strong contrast to the correlation in the light-cone coordinates, as seen from the Fourier transformation of the parton distribution in Feynman variable x , where the correlation length increases with the nucleon momentum. In the present formalism, the small x partons arise from

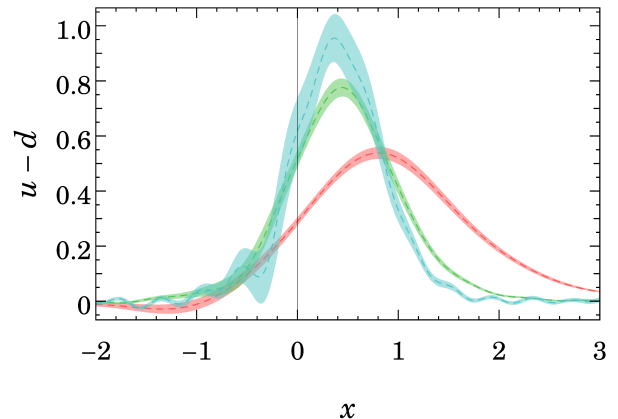


FIG. 1: The isovector quark quasi-distribution $\tilde{u}(x) - \tilde{d}(x)$ as defined in Eq. 1 computed on a lattice with the nucleon momentum P_z (in units of $2\pi/L$) = 1 (red), 2 (green), 3 (cyan).

the spatial correlation of order 1 fm, whereas the valence parton correlation is Lorentz contracted along the z direction, as discussed in Ref. [14].

We Fourier transform the z coordinate into momentum k to obtain the quasi-distribution $\tilde{q}_{\text{lat}}(x, \mu, P_z)$, which is shown in Fig. 1. It is quite striking that the peak at the lowest momentum is around $x = 1$, where the physical parton distribution vanishes. However, as the nucleon momentum doubles, the peak shifts to $x \approx 0.5$ and the value of the quasi-distribution at $x = 1$ reduces to half that of the peak. At the highest momentum, the peak is further shifted to $x \approx 0.4$ and the value at $x = 1$ is now about a third that of the peak. This is consistent with the expectation that as momentum becomes asymptotically large, the quasi-distribution becomes more similar to the physical parton distribution. However, there is a limitation the size of the momentum available on the lattice for nucleons. Therefore, LaMET must be used to extract the asymptotic distribution from the finite- P_z quasi-distributions. If we account for all the corrections, any quasi-distribution at a reasonably large P_z should yield the same physical prediction.

To take into account the one-loop corrections, we use the Z $\left(\xi = \frac{x}{y}, \frac{\mu}{P_z}, \frac{\Lambda}{P_z} \right)$ factor from Ref. [22]. To make the computation easier, we use the inverted Eq. 2 between the quasi- and physical distributions, expanded to linear order in α_s [17]. We take the UV cutoff Λ to be the largest lattice momentum π/a , and $\overline{\text{MS}}$ $\mu = 2$ GeV, which sets the scale of the parton distribution. The choice of the strong coupling is somewhat subtle.¹ Again, the Z factor

¹ In principle, one should use $6/(4\pi\beta)$ on the lattice; however, it is

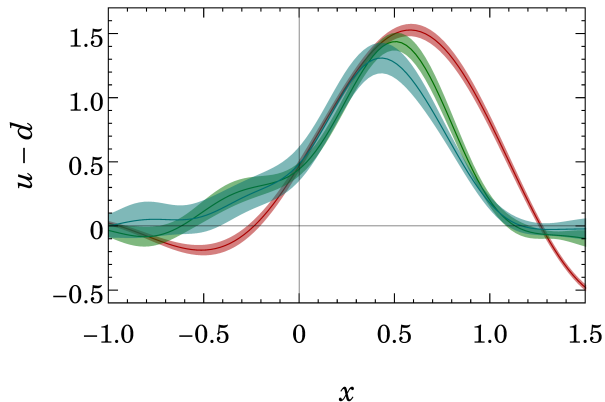


FIG. 2: The physical quark distribution $u(x) - d(x)$ extracted from Fig. 1 after making M_N^n/P_z^n corrections and one-loop corrections. The red, green and cyan bands correspond to $P_z \in \{1, 2, 3\} \frac{2\pi}{L}$. The two higher-momentum distributions are now almost identical.

from the cutoff scheme is correct to the leading logarithm but not for the numerical constant. This is a compromise that we make at the moment and will be rectified in the future.

At low nucleon momenta, the nucleon-mass corrections are as important as the one-loop correction, if not more. Using the operator product expansion, the nonlocal operator in Eq. 1 can be expanded as $\sum_{n=1}^{\infty} C_n(z) O_n(0)$, where the tree-level Wilson coefficient $C_n(z) = (iz)^{n-1} / (n-1)! + \mathcal{O}(\alpha_s)$ and $O_n(0) = \bar{\psi}(0) \gamma^z (iD^z)^{n-1} \psi(0)$. The tensor O_n is symmetric but not traceless, so it is a mixture of a twist-2 and higher-twist operators with the matrix element

$$\left\langle \vec{P} \left| O_n(0) \right| \vec{P} \right\rangle = 2a_n P_z^n K_n + \mathcal{O}(\Lambda_{\text{QCD}}^2 / P_z^2) \quad (4)$$

entirely expressible in terms of $a_n = \int dx x^{n-1} q(x)$, the n^{th} moment of the desired parton distribution, and $K_n = 1 + \sum_{i=1}^{i_{\text{max}}} C_i^{n-i} (M_N^2 / 4P_z^2)^i$ where C is the binomial function, and $i_{\text{max}} = \frac{n - (n \bmod 2)}{2}$. The $\mathcal{O}(\Lambda_{\text{QCD}}^2 / P_z^2)$ term is dynamical higher-twist correction. As one can see, the actual nucleon-mass correction parameter is $M_N^2 / 4P_z^2$.

After one-loop and nucleon-mass corrections, the resulting distributions are shown in Fig. 2. For the nuclear momenta under consideration, both types of correction are important. As one can see, the corrected distributions have much reduced P_z dependence, particularly for the two largest momenta. This suggests that

well known that this omits important tadpole contributions [15]. As a compromise, we take $\alpha_s = 0.20 \pm 0.04$, with the central value determined by the prescription of Ref. [15] and the uncertainty included as a part of the theoretical systematics.

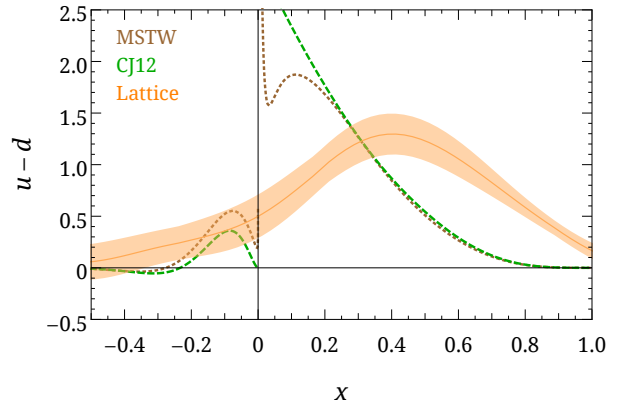


FIG. 3: The unpolarized isovector quark distribution $u(x) - d(x)$ computed on the lattice after extrapolation in P_z is shown as the purple band, compared with the global analyses by MSTW [18] (brown dotted line), and CTEQ-JLab (CJ12, green dashed line) [19] with medium nuclear correction near $(1.3 \text{ GeV})^2$. The negative x region is the sea quark distribution with $\bar{q}(x) = -q(-x)$. The lattice uncertainty band in the plot reflects the 68% C.L. The global fit uncertainty is not shown in the figure.

the corrections to the quasi-distributions will generate a P_z -independent physical distribution. The remaining small difference between the two large-momenta results could be due to the dynamical higher-twist corrections $\mathcal{O}(\Lambda_{\text{QCD}}^2 / P_z^2)$, which is expected to be smaller than the nucleon-mass effect. As for the lowest nucleon momentum (430 MeV) result, the LaMET expansion might not be very effective, although the peak after corrections has been shifted to near 0.8.

Finally, we find a P_z -independent distribution by taking into account the $\mathcal{O}(\Lambda_{\text{QCD}}^2 / P_z^2)$ correction by extrapolating using the form $a + b/P_z^2$. The final unpolarized distribution $u(x) - d(x)$ is shown in Fig. 3. The distribution for the $|x| > 1$ region is within 2 sigma of zero; thus, we recover the correct support for the physical distribution within error.

Our result cannot be directly compared with the experimental data because other lattice systematics are not yet under control. To obtain the physical parton distributions, we need to make a number of improvements, including reducing the quark masses to physical ones, increasing the number of configurations to reduce statistical errors, using finer lattice spacing to accommodate larger boosted momenta and improve the resolution, and using larger lattice volumes to access smaller x . Nonetheless, we hope that the present results do provide some insight into the qualitative features of the parton physics.

Also shown in Fig. 3 are the parton distributions from the global analyses by CTEQ-JLab (CJ12) [19] and NLO MSTW08 [18] at $\mu \approx 1.3 \text{ GeV}$. Note that the lattice re-

sults are not yet close to the physical pion mass, and the comparison with global analysis here is mainly to demonstrate the magnitude of the quantity, rather than to attempt to make a detailed comparison. The distribution in the mid- x region between 2 difference scales 1.3 GeV and 2 GeV is small, comparing with the changes we anticipate in the future calculation at physical pion mass. In Fig. 3, the lattice distribution weighs more at larger $|x|$. And since the total $u - d$ quarks are conserved, a reduction in small $|x|$ means an increase in larger $|x|$. This is also consistent with that the lattice first-moment of the momentum fraction ($\langle x \rangle_{u-d}$) and helicity ($\langle x \rangle_{\Delta u - \Delta d}$) above pion mass 250 MeV is roughly double the integrated values derived from global analyses [3, 16]. It would be very interesting to observe how the distribution changes when the lattice systematics improve.

The sea-quark distribution can be read from the negative- x contribution: $\bar{q}(x) = -q(-x)$. Our result favors a large asymmetry in the distributions of sea up and down antiquarks in the nucleon. There is a violation of the Gottfried sum rule with $\int_0^\infty dx (\bar{u}(x) - \bar{d}(x)) = 0.14(5)$, which was first observed by New Muon Collaboration (NMC) through the cross-section ratio for deep inelastic scattering of muons from hydrogen and deuterium [4], and later confirmed by other experiments using different processes, such as Drell-Yan at E665 [2] and E866/NuSea [21]. This is the first time we can demonstrate this directly from lattice QCD. Our result is close to the experimental one obtained by NMC in their DIS measurement, 0.147(39) at $Q^2 = 4 \text{ GeV}^2$ and by HERMES in their semi-inclusive DIS (SIDIS) result, 0.16(3) at $Q^2 = 2.3 \text{ GeV}^2$ [1].

The study of the isovector helicity distribution follows the same procedure with γ_z in Eq. 3 replaced by $\gamma_z \gamma_5$. Our result for antiquark helicity favors more polarized up quark than down flavor, while the total polarized sea asymmetry estimated by DSSV09 is consistent with zero within 2 sigma. We see a bigger polarized sea asymmetry, $\Delta \bar{u} - \Delta \bar{d} = 0.24(6)$, than the unpolarized case, as predicted in the large- N_c theory. We also see more weight distributed near the $x = 1$ regions, which could shift as we lower the light-quark masses in the future. In the near term, experiments in longitudinal single-spin asymmetry and parity-violating W production at RHIC might shed more light on the polarized sea distribution [5].

To summarize, we have presented a direct lattice-QCD calculation of the x dependence of parton distribution functions. By doing calculations with a large-momentum nucleon, we are able to connect light-cone quantities to lattice-QCD nonlocal but time-independent matrix elements. Since the largest attainable momentum is limited, we correct for the sizable finite-momentum dependence systematically. Our final result shows very encouraging signal for the isospin sea asymmetry in the unpolarized quark and helicity distributions. It is first time these are directly calculated with a first-principles nonperturba-

tive QCD approach. There is no fundamental difficulty in performing the calculation at the physical pion mass, and improving the statistical error to a level where we can compare with experiments quantitatively.

The LQCD calculations were performed using the Chroma software suite [11] on Hyak clusters at the University of Washington managed by UW Information Technology, using hardware awarded by NSF grant PHY-09227700. We thank MILC collaboration for sharing the lattices used to perform this study. The work of HWL and SDC is supported by the DOE grant DE-FG02-97ER4014 and DE-FG02-00ER41132. JWC is supported in part by the NSC, NTU-CTS, and the NTU-CASTS of R.O.C. The work of XJ is partially supported by the U. S. Department of Energy via grants DE-FG02-93ER-40762, and a grant (No. 11DZ 2260700) from the Office of Science and Technology in Shanghai Municipal Government, and by National Science Foundation of China (No. 11175114). HWL would like to thank the Shanghai Jiao Tong University for their hospitality during the development of the ideas presented in this work.

* Electronic address: hwlin@phys.washington.edu

† Electronic address: jwc@phys.ntu.edu.tw

‡ Electronic address: sdcohen@uw.edu

§ Electronic address: xji@umd.edu

- [1] K. Ackerstaff et al. The Flavor asymmetry of the light quark sea from semiinclusive deep inelastic scattering. *Phys.Rev.Lett.*, 81:5519–5523, 1998.
- [2] M.R. Adams et al. Extraction of the ratio $F2_n/F2_p$ from muon - deuteron and muon - proton scattering at small x and Q^{*2} . *Phys.Rev.Lett.*, 75:1466–1470, 1995.
- [3] C. Alexandrou, M. Constantinou, V. Drach, K. Hatziyiannakou, K. Jansen, et al. Nucleon Structure using lattice QCD. *Nuovo Cim.*, C036(05):111–120, 2013.
- [4] M. Arneodo et al. A Reevaluation of the Gottfried sum. *Phys.Rev.*, D50:1–3, 1994.
- [5] E.C. Aschenauer, A. Bazilevsky, K. Boyle, K.O. Eysler, R. Fatemi, et al. The RHIC Spin Program: Achievements and Future Opportunities. 2013.
- [6] A. Bazavov et al. Lattice QCD ensembles with four flavors of highly improved staggered quarks. *Phys.Rev.*, D87(5):054505, 2013.
- [7] Tanmoy Bhattacharya, Saul D. Cohen, Rajan Gupta, Anosh Joseph, Huey-Wen Lin, et al. Nucleon Charges and Electromagnetic Form Factors from 2+1+1-Flavor Lattice QCD. *Phys.Rev.*, D89:094502, 2014.
- [8] Wen-Chen Chang and Jen-Chieh Peng. Flavor Structure of the Nucleon Sea. 2014.
- [9] Daniel de Florian, Rodolfo Sassot, Marco Stratmann, and Werner Vogelsang. Extraction of Spin-Dependent Parton Densities and Their Uncertainties. *Phys.Rev.*, D80:034030, 2009.
- [10] Dmitri Diakonov and V. Yu. Petrov. Chiral Theory of Nucleons. *JETP Lett.*, 43:75–77, 1986.
- [11] Robert G. Edwards and Balint Joo. The Chroma soft-

- ware system for lattice QCD. *Nucl.Phys.Proc.Suppl.*, 140:832, 2005.
- [12] Anna Hasenfratz and Francesco Knechtli. Flavor symmetry and the static potential with hypercubic blocking. *Phys.Rev.*, D64:034504, 2001.
- [13] Xiangdong Ji. Parton Physics on Euclidean Lattice. *Phys.Rev.Lett.*, 110:262002, 2013.
- [14] Xiangdong Ji. Parton Physics from Large-Momentum Effective Field Theory. *Sci.China Phys.Mech.Astron.*, 57:1407–1412, 2014.
- [15] G. Peter Lepage and Paul B. Mackenzie. On the viability of lattice perturbation theory. *Phys.Rev.*, D48:2250–2264, 1993.
- [16] Huey-Wen Lin. A Review of Nucleon Spin Calculations in Lattice QCD. *AIP Conf.Proc.*, 1149:552–557, 2009.
- [17] Yan-Qing Ma and Jian-Wei Qiu. Extracting Parton Distribution Functions from Lattice QCD Calculations. 2014.
- [18] A.D. Martin, W.J. Stirling, R.S. Thorne, and G. Watt. Parton distributions for the LHC. *Eur.Phys.J.*, C63:189–285, 2009.
- [19] J.F. Owens, A. Accardi, and W. Melnitchouk. Global parton distributions with nuclear and finite- Q^2 corrections. *Phys.Rev.*, D87:094012, 2013.
- [20] J. Speth and Anthony William Thomas. Mesonic contributions to the spin and flavor structure of the nucleon. *Adv.Nucl.Phys.*, 24:83–149, 1997.
- [21] R.S. Towell et al. Improved measurement of the anti-d / anti-u asymmetry in the nucleon sea. *Phys.Rev.*, D64:052002, 2001.
- [22] Xiaonu Xiong, Xiangdong Ji, Jian-Hui Zhang, and Yong Zhao. One-Loop Matching for Parton Distributions: Non-Singlet Case. *Phys.Rev.*, D90:014051, 2014.